JMBFS

Journal of Microbiology, Biotechnology and Food Sciences

International peer-reviewed scientific online journal

Published by Faculty of Biotechnology and Food Sciences

IMMOBILIZATION OF MICROORGANISMS ON SOLID SORBENTS OF A NEW GENERATION OBTAINED ON THE BASIS OF ALUMINUM OXIDE VIA MICRO-ARC OXIDATION

Zakhro Akhmedova[1], Anatoliy Tonkikh[1], Tulkin Shonakhunov[1], Abdulaziz Ibragimov[1], Munavvar Yakhyaeva[1], Ziyoda Khamraeva[1], Iroda Gulyamova[1], Gulchekhra Kadirova[1], Olga Verushkina[1]*

Address(es):
[1] Institute of Microbiology, Academy of Sciences of the Republic of Uzbekistan, 7B A. Kadiri Street, 100128 Tashkent, Uzbekistan, +998 71 241 71 20.

*Corresponding author: akhmedovazr@mail.ru

https://doi.org/10.55251/jmbfs.14060

ARTICLE INFO

Received 6. 3. 2026
Revised 27. 3. 2026
Accepted 29. 4. 2026
Published 1. 6. 2026

Regular article

OPEN ACCESS

ABSTRACT

This study presents experimental data on the sorption of microorganisms onto composite ceramic coatings formed on aluminum alloys (Zn–Al, Al–Mg6, and D16) via micro-arc oxidation (MAO). The tested microorganisms included *Escherichia coli*, *Pseudomonas aeruginosa*, *Bacillus subtilis*, *Staphylococcus aureus*, the yeast-like fungus *Candida albicans*, and the micromycete *Aspergillus niger*. The results demonstrated that the sorption capacity of the coatings is strongly influenced by microbial species, as well as by the chemical composition and surface morphology of the sorbents. Scanning electron microscopy (SEM) revealed a heterogeneous distribution of adsorbed cells and spores, governed by microporosity, phase composition (oxides of aluminum, magnesium, zinc, and silicon), and surface structural features. The maximum sorption of *E. coli* on the Zn–Al coating reached 0.9×10^6 cells/mm² at an concentration of 3×10^8 cells/mL, exceeding that observed on the D16 alloy by 30%. Comparable trends were observed for *P. aeruginosa* and *B. subtilis*. Coccoid cells of *S. aureus* also exhibited efficient adsorption, with densities of 1.80×10^6 cells/mm² on Zn–Al, 1.50×10^6 cells/mm² on D16, and 1.30×10^6 cells/mm² on Al–Mg6 surfaces. At higher microbial concentrations ($\geq 3 \times 10^8$ cells·cm^{-3}), the maximum surface sorption density reached $7.0–8.0 \times 10^5$ cells/mm². Yeast cells of *C. albicans* and spores of *A. niger* exhibited adsorption behavior similar to that of *S. aureus*. The highest sorption capacity was consistently observed for Zn–Al coatings, followed by D16, while lower values were recorded for Al–Mg6 and control samples. Overall, MAO-derived composite coatings demonstrated high porosity and significant sorption capacity, indicating their strong potential as adsorbents and carrier materials in industrial microbiology, biotechnology, and environmental monitoring. Furthermore, these coatings represent promising candidates for future investigations of antimicrobial and anticorrosion properties.

Keywords: Aluminum oxide, microarc oxidation coatings, aluminum alloys, microbial adhesion, electron microscopy, degrees of adsorption

INTRODUCTION

One of the most promising approaches for enhancing the surface properties of machine components and metallic structures, particularly in terms of resistance to corrosion induced by physicochemical factors and microbial degradation, is micro-arc oxidation (MAO), also referred to as plasma electrolytic oxidation (PEO). These advanced surface engineering technologies are widely applied for the modification of metals and alloys, aiming to improve their corrosion resistance and extend their applicability in industrial environments (**Davis, 2001; Suminov *et al*., 2011**).

The application of these approaches enables the formation of ceramic coatings on valve metals (such as Al, Ti, Zr, Nb, and Mg) and their alloys. The resulting coatings are characterized by high hardness, mechanical strength, corrosion resistance, wear resistance, and significant sorption capacity. These properties have led to their widespread implementation across various industrial sectors, including mechanical engineering, instrumentation, microelectronics, the oil and gas industry, aerospace engineering, and biotechnology (**Suminov *et al*., 2011; Gupta, 2018**).

However, despite the well-documented mechanical and anticorrosion advantages of MAO-derived coatings, the sorption properties imparted to modified alloys and their adsorption behavior toward different classes of microorganisms—including potential infectious agents—remain insufficiently investigated. In addition, their potential inhibitory and/or antimicrobial activity has not yet been comprehensively elucidated (**Wen *et al*., 2023; Lemire *et al*., 2013**).

During the MAO process, the component is immersed in a specially prepared electrolyte solution and connected to the positive terminal (serving as the anode), while the electrolyte is linked to the negative terminal via a stainless-steel electrode. Upon application of a constant voltage (approximately 200 V), anodization occurs, resulting in the formation of an oxide film on the metal surface. Subsequently, a pulsed voltage (approximately 300–700 V) is applied, inducing numerous micro-arc (plasma) discharges between the surface and the electrolyte. These discharges significantly increase the thickness of the oxide layer (up to 400 μm) and lead to the formation of a robust, porous, and electropositive coating (**Borisov *et al*., 2016**).

Depending on the selected MAO processing parameters (voltage, pulse frequency, and electrolyte composition), coatings with diverse functional properties can be obtained. For instance, the incorporation of silver, copper, or zinc ions into the electrolyte facilitates the formation of surfaces with pronounced bactericidal activity (**Komarov *et al*., 2024; Manikandan *et al*., 2019**).

MAO-treated aluminum surfaces are characterized by high porosity and are presumed to exhibit enhanced adsorption capacity due to the electropositive charge of the formed oxide layer (**Suminov *et al*., 2011; Gupta, 2018**). Nevertheless, studies addressing microbial adsorption onto solid coatings produced by MAO remain limited. For example, Giardia lamblia cysts and Ascaris lumbricoides eggs were comparatively evaluated for sorption on MAO-derived aluminum oxide coatings and on Al_2O_3 sorbents in powder, granular, and cylindrical forms (**Karamysheva *et al*., 2019**). The highest sorption capacity was observed for MAO-coated surfaces, reaching 86.5% adsorption for *A. lumbricoides* eggs and 55.2% for *G. lamblia* cysts. In comparison, Al_2O_3 granules (0.4–1.2 μm) exhibited moderate adsorption efficiencies (35.4% and 47.5%, respectively), whereas other forms of Al_2O_3 demonstrated sorption levels not exceeding 10%.

It should be noted that the high sorption capacity of solid surfaces, particularly with respect to microorganisms, may have significant practical implications (Abdullaev, 2023; Srinivasan *et al*., 2015). For instance, microbial sorption onto solid materials can be applied in environmental monitoring of microbial contamination in air and water, as well as in modern biotechnological processes, including food production, soil remediation, and the treatment of wastewater contaminated with pesticides and other pollutants. Additionally, such systems are relevant for strategies aimed at corrosion prevention (Suryavanshi *et al*., 2017). The immobilization of microorganisms on solid surfaces is considered a promising approach, as immobilized cells are known to retain their biological activity for significantly longer periods compared to planktonic (suspended) cells (**Pishchikov & Minukhin, 2017; Subramaniam *et al*., 2019; Li *et al*., 2022; Zhang *et al*., 2020**).

Since there is only one study in the literature on the adsorption of relatively large ascaris eggs (50-100 μm) and lamblia cysts (10 μm) on an MDO aluminum coating, we hypothesize that composite coatings will be effective sorbents for many types of microorganisms and on this basis they will be promising sorbents in the field of microbiology, biotechnology and industry.

In this context, the aim of the present study was to investigate the sorption and desorption behavior of selected indicator microorganisms—widely used for assessing environmental contamination—on three types of composite microplasma aluminum coatings (Zn–Al, Al–Mg6, and D16) produced via micro-arc oxidation (MAO) at the Joint Institute of Mechanical Engineering of the National Academy of Sciences of Belarus (**Komarov *et al*., 2024**).

MATERIALS AND METHODS

Characterization of Aluminum Coating Samples

Aluminum plates with composite coatings (Zn–Al, Al–Mg6, and D16) were fabricated at the Joint Institute of Mechanical Engineering of the National Academy of Sciences of Belarus and kindly provided by A.I. Komarov (**Komarov *et al*., 2024**).

The D16 coating, formed on an aluminum alloy substrate (D16), consisted predominantly of the hexagonal γ-Al_2O_3 phase, which is known to exhibit bactericidal properties. The coating was composed mainly of γ-Al_2O_3 (~70%), with pore sizes ranging from 0.5 to 5 μm (up to 20 μm in some regions), a thickness of 60–70 μm, and a porosity of 40–50%. The total surface area of the plates (both sides) was 19.8 cm^2.

The Al–Mg6 coating (formed on an AlMg6 alloy substrate) consisted of a combination of cubic α-Al_2O_3 (a stable and non-toxic phase) and γ-Al_2O_3 in a ratio of 70% and 30%, respectively. The coating thickness ranged from 60 to 70 μm, with a porosity of 40–50%. The pore size distribution was 0.5–5 μm, reaching up to 20 μm at agglomerate boundaries. The depth of the porous layer was approximately 20 μm. The total surface area of the plates was 20.5 cm^2.

The Zn–Al coating was a composite consisting of α-Al_2O_3, ZnO, $ZnAl_2O_4$, and mullite ($3Al_2O_3 \cdot 2SiO_2$; $Al_6Si_2O_{13}$). This coating was characterized by the presence of large pores (10–30 μm) in combination with smaller pores (1–3 μm). The coating thickness was 60–70 μm, and the total surface area of the plates was 23.4 cm^2.

Control samples consisted of aluminum plates (3.3 × 3.3 × 0.1 cm; total surface area of 20 cm^2) coated with immobilized Al_2O_3 powder (particle size 20–200 μm) using cyanoacrylate adhesive (Akfix 705, AKKIM, Turkey). After application of excess powder and polymerization, the plates were washed with ethanol and distilled water prior to use.

Preparation of Microbial Cell Suspensions

Microbial strains obtained from the collection of the Institute of Microbiology of the Academy of Sciences of the Republic of Uzbekistan were used in this study, including *Escherichia coli*, *Bacillus subtilis*, *Pseudomonas aeruginosa*, *Staphylococcus aureus*, *Candida albicans*, and *Aspergillus niger*.

Bacterial strains were cultivated in nutrient broth for 24 h at 37 °C with agitation at 160 rpm. The cells were harvested by vacuum filtration using nitrocellulose membranes (pore size 0.45 μm), followed by washing with phosphate-buffered saline (PBS, 1 mM, pH 7.4) and physiological saline solution. The resulting cell suspensions were adjusted to the desired concentrations.

Cell viability during storage at room temperature (24 °C) decreased by approximately 15% within 90 min; therefore, this time interval was considered acceptable for experimental procedures.

All experimental procedures involving *Pseudomonas aeruginosa*, *Staphylococcus aureus*, and *Candida albicans* were conducted in compliance with Biosafety Level 2 (BSL-2) requirements using a certified biological safety cabinet.

Candida albicans and *Aspergillus niger* were cultivated on Sabouraud agar under standard conditions. Following sporulation and mycelial growth, spores were harvested by washing with phosphate buffer. The spore suspensions were separated from mycelial fragments by filtration through sterile filter paper ("Blue Ribbon") under aseptic conditions and subsequently diluted in phosphate buffer to the required concentrations.

In a separate experiment, the viability of filtered cells was assessed during storage at 24 °C for periods ranging from 3 to 24 h prior to immobilization experiments. It was observed that after 90 min of storage, the number of viable cells decreased by approximately 15%. Therefore, a storage period of up to 90 min was considered acceptable for subsequent experimental procedures.

Determination of Cell Concentration

Cell concentration was determined either by direct microscopic counting using a Goryaev counting chamber or by measuring optical density at 550 nm (OD_{550}), calibrated against McFarland turbidity standards (**Mahesh *et al*., 2025**). The applied calibration range corresponded to approximately 1.0×10^8 to 3.0×10^9 CFU/mL (0.5–10 McFarland units).

For each microbial culture, calibration curves were established to correlate optical density values with cell concentration. This approach enabled the subsequent use of spectrophotometric measurements as a reliable method for routine quantification.

Quantification of Microorganisms on Opaque Surfaces

Aluminum plates with adsorbed microorganisms were air-dried, fixed with methanol, and subsequently dried again. The samples were then stained with 0.01% acridine orange by immersion for 2 min. Stained specimens were examined under reflected light using a fluorescence microscope (Carl Zeiss Primostar 3, Germany) with excitation at 470 nm (**Hobbie *et al*., 1977**).

Using this method, reliable enumeration of fluorescent cells was achieved only when their surface density did not exceed 20,000 cells per mm^2. Therefore, this approach was primarily applied to quantify the number of microorganisms remaining on the plates after desorption in 1.0 mM phosphate buffer.

Sorption of Microorganisms on Coated Plates

Adsorption of washed bacterial cells and fungal spores was performed by immersing the plates individually in 50 ml of suspension (concentration 10^6 – 6×10^8 cells/ml) in PBS and incubating for 30 min at 25°C with shaking. The number of adsorbed cells was calculated based on the difference in microorganism concentrations in the suspension before and after incubation. The number of adsorbed cells per mm^2 was calculated based on the known surface area. In addition, the actual number of adsorbed cells on the sorbent surface was estimated using electron microscopy. Cell/spore adsorption was assessed in four independent biological replicates. Separate samples for each material were prepared on different days. For each suspension sample, cells/spores were counted in 10–15 random fields of view (technical replicates). The average value for the technical replicates was used to calculate the mean and standard deviation for the biological replicates. After desorption, the plates were dried, fixed with methanol, stained with 0.01% acridine orange (2 min), and examined under a fluorescence microscope (Carl Zeiss Primostar, Germany, excitation 470 nm) (Hobbie *et al*., 1977). Reliable counting is possible up to 20,000 cells/mm^2.

Desorption Procedure

Aluminum plates with adsorbed microorganisms were immersed in 1 L of 1 mM phosphate-buffered saline (PBS) and subjected to continuous stirring using a magnetic stirrer until the concentration of microorganisms in the solution reached equilibrium (typically 20–30 min).

Subsequently, the plates were removed and transferred into a fresh 1 L portion of 1 mM PBS, followed by an additional 30 min of magnetic stirring. After completion of the desorption process, the plates were retrieved, air-dried, fixed with methanol, and stained with acridine orange. The number of residual microorganisms remaining on the surfaces was then quantified using fluorescence microscopy, as described above.

Zeta Potential Measurement of Bacterial Cells

The zeta potential of bacterial cells was measured using a Delsa Nano Particle Analyzer (Beckman Coulter Inc., USA). Measurements were performed by electrophoretic light scattering at a detection angle of 30°, based on the analysis of particle mobility in an applied electric field.

Preparation of Samples for Scanning Electron Microscopy (SEM)

Samples with adhered microorganisms were fixed in 2.5% glutaraldehyde prepared in phosphate buffer (pH 7.2). Following fixation, the samples were dehydrated through a graded ethanol series (30–100%) and subsequently subjected to critical point drying using CO_2. The dried samples were coated with a thin layer of gold/platinum to improve conductivity, although in some cases imaging was performed without sputter coating due to the use of a conductive substrate. The specimens were examined using a JEOL JSM-2100 (JEOL, Japan) at accelerating voltages with magnifications of ×3000 and ×5000. SEM analysis was carried out at the Laboratory of Physics and Physicochemical Methods of Investigation, Institute of Physics and Chemistry of Polymers of the Academy of Sciences of the Republic of Uzbekistan.

Statistical Analysis

Experiments were performed in 3-4 biological replicates, each with at least 6 technical replicates. Statistical analysis was performed in Microsoft Excel 2007. Graphs were generated using Origin 6.1. Differences were considered significant at $p < 0.05$. SD (±10 million cells/mL). Due to the relatively low precision of cell concentration measurements based on turbidity in the range of 50–600 million cells/mL (±10 million cells/mL), the standard deviation for some values was relatively high. However, this level of precision was considered sufficient for a preliminary estimate of the maximum cell density on MAO-coated plates.

RESULTS AND DISCUSSION

Properties of Composite Ceramic Coatings Obtained by MAO on Aluminum Alloys

Figure 1 (A–C) presents the X-ray diffraction (XRD) patterns illustrating the phase composition of the coatings formed on different aluminum alloys. The coating obtained on the D16 alloy (Fig. 1A) was predominantly composed of α-Al_2O_3, accounting for approximately 75 wt.%. In contrast, the coating formed on the Al–Mg6 alloy (Fig. 1B) consisted mainly of γ-Al_2O_3 (~90 wt.%), indicating a distinct phase composition compared to D16. The coating produced on the Zn–Al alloy (Fig. 1C) exhibited a more complex phase structure. The dominant phase was zinc aluminate ($ZnAl_2O_4$), accompanied by α-Al_2O_3 and mullite ($2Al_2O_3 \cdot 3SiO_2$).

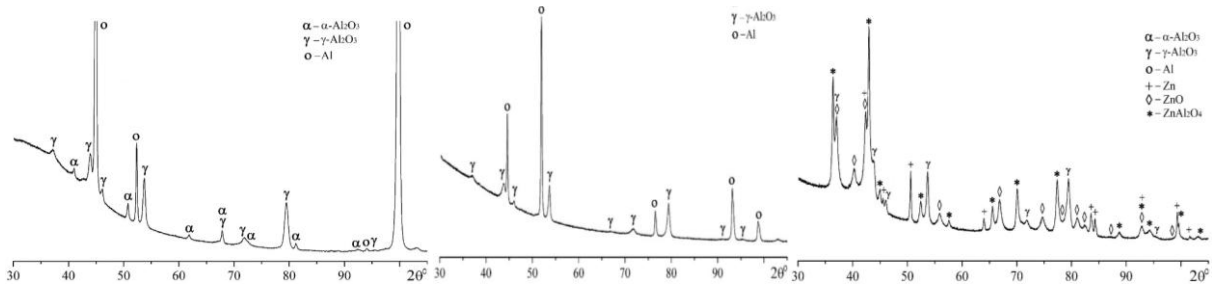

Figure 1 X-ray diffraction (XRD) patterns of ceramic coatings formed on aluminum alloys: D16 (A), Al–Mg6 (B), and Zn–Al (C).

As shown in Figure 1, the coatings are primarily composed of aluminum oxides in different polymorphic forms, the relative proportions of which depend on both the chemical composition of the alloy and the parameters of the micro-arc oxidation (MAO) process (Marek Szkodo *et al*., 2021). In addition to phase composition, the coatings exhibit a porous structure, with pore size and distribution also governed by MAO processing conditions. These characteristics confer significant functional advantages to MAO-derived coatings, making them promising materials for the separation of multicomponent systems, selective adsorption, and various applications in chemistry, microbiology, and engineering. Aluminum oxide is generally regarded as an electropositive sorbent, meaning that its surface possesses an excess positive charge. This charge is believed to arise from surface dehydration processes, involving the removal of water molecules and the formation of coordinatively unsaturated aluminum atoms. These sites, characterized by localized positive charge, are commonly referred to as Lewis acid centers (**Romanova and Petrova, 2006**).

Sorption of Microorganisms on MAO-Coated Aluminum Surfaces

To determine the optimal incubation time required for adsorption equilibrium between microorganisms adsorbed on aluminum plates and those remaining in suspension, a kinetic experiment was conducted. Three beakers were prepared, each containing 50 ml of an E. coli suspension at a concentration of 1×10^7 cells ml^{-1}. An aluminum plate with one type of composite coating (AlMg6, Zn–Al, or D16) was immersed in each beaker. The suspensions were stirred using a magnetic stirrer, and samples were taken every 5 minutes to determine the residual cell concentration in the solution. As shown in Figure 1, adsorption equilibrium between the porous surface of the coatings and the bacterial cells in suspension was achieved after 20–30 minutes of stirring. Therefore, in all subsequent experiments, the incubation time for cell adsorption on the studied sorbents was standardized to 30 minutes.

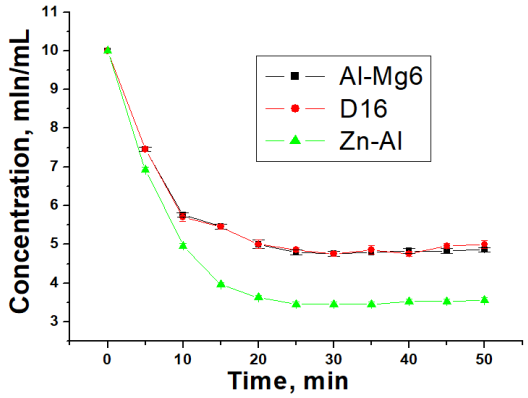

Figure 2 Dependence of *Escherichia coli* cell concentration in the suspension on the incubation time with composite-coated aluminum plates. Values represent the mean of three independent experiments, with standard deviations not exceeding 0.05 and therefore smaller than the symbol size.

Next, the adsorption of E. coli bacteria on four types of aluminum plates was studied as a function of cell concentration in the solution. The results showed that, over the concentration range from 1×10^6 to 5×10^7 cells cm^{-3}, the adsorption percentage increased linearly with increasing cell concentration.

At higher concentrations (≥3×10^8 cells cm^{-3}), saturation of the plate surfaces was observed, with a maximum surface density of approximately 700,000–800,000 cells/mm^2.

Notably, MAO-treated surfaces adsorbed several times more bacterial cells compared to control plates coated with bonded alumina powder (Figure 3.1), indicating the superior adsorption capacity of coatings produced by microarc oxidation.

A similar adsorption pattern was observed for *P. aeruginosa* (Fig. 3.2) and *B. subtilis* (Fig. 3.3). In both cases, adsorption increased with increasing cell concentration in the suspension and reached saturation at high concentrations.

Gram-positive cocci *S. aureus* were also effectively adsorbed onto aluminum alloy surfaces at a suspension concentration of approximately 3×10^8 cells mL^{-1}. However, their adsorption density was significantly higher compared to previously tested bacteria: approximately 1,800,000 cells/mm^2 on Zn–Al plates, 1,500,000 cells/mm^2 on D16 plates, and 1,300,000 cells/mm^2 on Al–Mg6 plates (Fig. 3.4).

Spherical yeast cells of *C. albicans* (Fig. 3.5) exhibited a comparable adsorption pattern to that observed for *S. aureus*, with the highest sorption densities on the Zn–Al and D16 coatings and slightly lower values on the Al–Mg6 coating.

On control plates coated with bonded alumina powder, spore adsorption was significantly lower (Fig. 3.5).

A. niger spores exhibited adsorption behavior similar to that of C. albicans (Fig. 3.6).

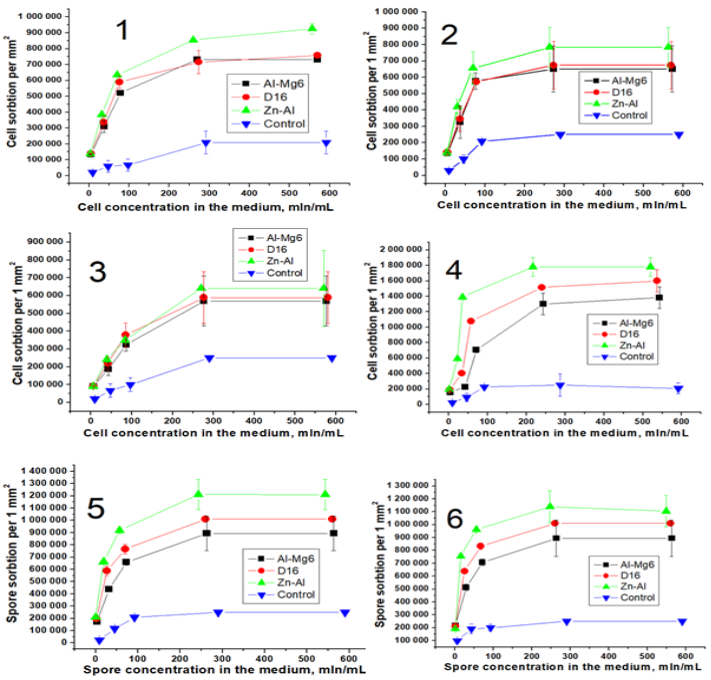

Figure 3 Relationship between cell concentration in suspension and surface adsorption density on different composite coatings (Zn–Al, D16, and Al–Mg6) and immobilized Al_2O_3 powder (control). (1) *Escherichia coli*; (2) *Pseudomonas aeruginosa*; (3) *Bacillus subtilis*; (4) *Staphylococcus aureus*; (5) *Candida albicans*; (6) *Aspergillus niger*. Values represent the mean of three independent experiments with standard deviations indicated.

Analysis of Sorption Curves

The purpose of experiments on the adsorption of microorganisms with MAO coatings on aluminum plates is to obtain information on the maximum number of microorganisms capable of adsorption per unit plate area (Gmax) and the microorganism concentration at which all binding sites on the coating are saturated (K). Since it is difficult to accurately determine the concentration of microorganisms saturating the sites, the sorbate concentration at which half of the binding sites on the sorbent are occupied has been considered the sorbate characteristic. For this purpose, several mathematical transformations of the adsorption curve were developed, converting the curve into a straight line.

The hyperbolic shape of the binding site saturation curves for microorganisms on the adsorbent (adsorption isotherms) in Figure 2 suggests that these curves may obey certain adsorption laws. There is no single theory that would accurately describe the adsorption of various substances (especially microorganisms) on different surfaces. The adsorption isotherms we obtained are similar to Langmuir or Freundlich isotherms for monomolecular adsorption of a solution on a solid (**Liu and Wang, 2009; Danat *et al*., 2026**), as well as to ligand-receptor binding curves, assuming a single receptor type and enzymatic reaction kinetics. Many mathematical transformations have been proposed for analyzing hyperbolic curves, converting them into straight lines. Double-inverse Langmuir coordinates, double-logarithmic Freundlich coordinates, and others have been proposed for analyzing adsorption isotherms. Plots in Scatchard coordinates, double-inverse Lineweaver-Burk coordinates, and several other coordinate systems have been proposed for studying ligand binding to receptors.

We plotted the adsorption isotherms we obtained in some of these coordinates (Fig. 4).

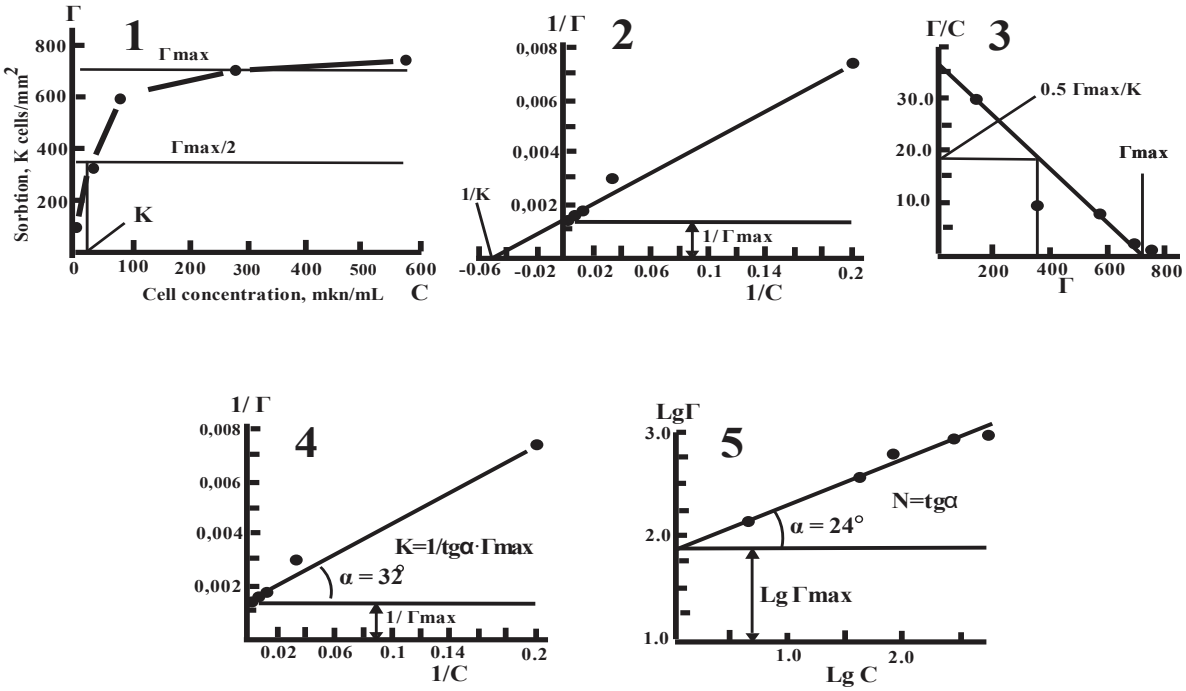

Figure 4 Adsorption isotherm of *E. coli* on D16 coating in direct coordinates (1), double-inverse Lineweaver-Burk coordinates (2), Scatchard coordinates (3), double-inverse Langmuir coordinates (4), and double-log Freundlich coordinates (5).

Conversion of the adsorption isotherm of *E. coli* on D16 coating (Fig. 4.1) to double-inverse Lineweaver-Burk coordinates (Fig. 4.2) showed a maximum adsorption Gmax of 700,000 cells/mm^2 and a cell concentration at half-saturated sites K 20,000 cells/mL.

Transformation of the adsorption isotherm into Scatchard coordinates (Fig. 4.3) also revealed $\Gamma_{max} \approx$ 700,000 cells/mm2 and K ≈ 350,000 / 18 ≈ 19,400 cells/mL, i.e., a value equal to K, within the error limits, as obtained in double-inverse coordinates.

In ligand-receptor binding experiments, the ligand concentration at half the bound (saturated) sites is called the ligand affinity constant for the receptor, or dissociation constant (K_D). The lower the K_D, the higher the affinity. For microorganisms, the lower this constant, the higher the affinity of the microorganisms for the sorbent surface, since microorganisms will saturate the sorbent at lower concentrations.

In Langmuir's double-inverse coordinates (Fig. 4.4), the maximum adsorption is also $\Gamma_{max} \approx$ 700,000 cells/mm^2, but to characterize the adsorption process, Langmuir introduced the adsorption equilibrium constant (K_L) equal to $K_L = 1/tg\ 32° \times \Gamma_{max} = 1/0.62 \times 700{,}000 = 1/434{,}000 = 2.3 \times 10^{-6}$. With regard to microorganisms, the higher the K_L, the greater the affinity of the microorganisms for the sorbent surface.

Freundlich showed that, at a constant temperature, the number of moles of dissolved substance per unit mass of adsorbent (Γ) is proportional to the equilibrium concentration (C) of the adsorbent, raised to a certain power, which is usually less than unity. $\Gamma = \Gamma_{max} \times CN$, where Γ_{max} is the maximum adsorption density, and N is an empirical constant characteristic of a given adsorption process within certain limits. N characterizes the curvature of the adsorption isotherm and typically has values from 0.1 to 0.6. The higher N, the greater the affinity of the sorbate for the sorbent.

In double logarithmic coordinates of the adsorption isotherm (Fig. 6.4), $Lg\ \Gamma_{max} \approx$ 1.85, where $\Gamma_{max} \approx$ 700,000 cells/mm^2, N = tg 24° ≈ 0.44

As can be seen from Fig. 4, in all graphical transformations of the adsorption isotherm, one can obtain the value of the maximum adsorption capacity of a solid and a constant characterizing the ability of the sorbate to be sorbed on the sorbent. Based on the above data, it can be concluded that the concepts of ligand-receptor interactions are also suitable for the analysis of microorganism sorption on solid surfaces.

The hyperbolic curves we obtained for the dependence of microorganism concentration on their adsorption fit well with the theory of molecular ligand-receptor interactions and the theory of adsorption of gas and solute molecules on a solid sorbent. However, due to their large size, microorganism adsorption, strictly speaking, does not correspond to molecular adsorption mechanisms.

Ligand-receptor interaction theories are based on the equilibrium binding of one ligand molecule with high affinity to one receptor molecule. Langmuir's adsorption theory is based on the following: adsorption does not occur across the entire surface of the adsorbent, but rather at homogeneous, identical, and independent active sites (sites); each active site is capable of interacting with only one adsorbate molecule; as a result, only a single layer of adsorbed molecules can form on the surface.

Microorganisms have a large number of molecules on their surface, capable of simultaneously binding to many active sites on the sorbent. Microorganisms vary in size, so in our case, the binding density of small, spherical S. aureus is almost twice that of large, rod-shaped bacteria such as E. coli, P. aeruginosa, and B. subtilis. The low accuracy of measuring cell concentration using optical turbidity and microscopic methods prevents us from deriving mathematical relationships between microorganism size, maximum density of adsorbed microorganisms, and their affinity for the sorbent. This is a topic for future research. Here, we merely outline a path to solving this problem.

Microorganism Desorption Study

For the desorption study, microorganism-laden plates were immersed in 0.1 L of phosphate-buffered saline (PBS, pH 7.4) and stirred with a magnetic stirrer. As a result, the microorganism concentration in the solution increased due to desorption from the sorbent surface, reaching approximately 10^6 cells/mL.

To ensure complete desorption, the plates were additionally washed several times in 0.1 L of fresh PBS to ensure maximum elution of bacterial cells and fungal spores. After desorption, the plates were dried, fixed with methanol, and stained with acridine orange. Fluorescence microscopy analysis of all ceramic-coated aluminum plates revealed that residual amounts of tightly bound microbial cells and spores remained on the surfaces (Table 1). These cells and spores likely penetrated pores and microcracks in the oxide coatings or were firmly bound to the sorbent, preventing their complete removal during rinsing.

Table 1 Residual microorganism counts on Petri dishes after desorption with PBS, as determined by fluorescence microscopy.

Microorganisms	Al-Mg6, cell/mm^2	D16, cell/mm^2	Zn-Al, cell/mm^2	Glued Al_2O_3, cell/mm^2
E. coli	2147±24	2355±60	3974±161	646±84
P. aeruginosa	2086±29	2136±29	3111±54	556±65
B. subtilis	1968±95	2015±70	2507±103	456±94
S. aureus	3891±173	4523±140	5421±354	730±90
C. albicans (spores)	3230±155	3695±117	4911±101	586±46
A. niger (spores)	3363±56	3627±91	4821±63	577±25

The mean values and standard errors are presented for four independent experiments.

The almost complete desorption of microorganisms during elution indicates that adsorption is equilibrium and reversible. That is, the adsorbed microorganism is retained by the active site for a period of time, after which it is desorbed. After some time, a dynamic equilibrium is established between the adsorption and desorption processes, where the adsorption rate equals the desorption rate. The mechanism of equilibrium adsorption is determined primarily by physical factors, including the electrical charges of the microorganism and sorbent surfaces, their hydrophobicity, porosity, and other factors.

Zeta potential of microbial cells.

The sorption properties of aluminum oxides for various microorganisms depend on many factors: surface roughness, pore size, electrical charge, hydrophobicity or hydrophilicity, as well as substances secreted by microorganisms, etc. However, the main contribution to the high efficiency of bacterial retention by aluminum oxide is the electrostatic interaction between the cell and the adsorbent, caused by the presence of oppositely charged functional groups on the interacting surfaces. Moreover, microbial cell surfaces under physiological conditions are predominantly negatively charged (**Ferreyra Maillard *et al*., 2021**), and aluminum oxide is primarily an electropositive sorbent due to the excess concentration of Lewis acid sites (LAS), which are coordinatively unsaturated surface aluminum atoms with a localized positive charge (**Romanova *et al*., 2006**). Direct determination of cell surface charge is very difficult, but it can be calculated from the electrokinetic or zeta (ζ) potential of the cells, which is relatively easy to measure using electrophoretic cell mobility. Zeta (ζ) potential is measured in a special electrophoretic chamber, where the velocity of cell movement is measured at a specific electric field strength using the Einstein-Smoluchowski formula. Specialized instruments for measuring zeta potential exist. In these instruments, cell velocity is measured using a laser Doppler anemometer, which is based on the change in the frequency of laser light scattered by moving particles (**Ferreyra Maillard *et al*., 2021**).
The results of zeta potential measurements for the studied microorganisms are presented in Table 2. As expected, the zeta potentials of all cells are negative and depend on the composition of the solution. At higher solution concentrations, the zeta potentials are lower.

Table 2 Zeta potentials of cells at two concentrations of phosphate buffer solution with pH = 7.4. Mean values and standard errors are presented for the results of 4 experiments.

Microorganisms	Zeta potential at 1 mM PBS, pH=7.4, mV	Zeta potential at 100 mM PBS, pH=7.4, mV
E. coli	— 52,2 ± 6,4	— 28,7 ± 3,3
B. subtilis	— 42,7 ± 5,5	— 22,6 ± 3,1
S. aureus	— 46,5 ± 5,0	— 26,5 ± 3,4
P. aeruginosa	— 37,4 ± 4,2	— 18,5 ± 2,4
C. albicans (spores)	— 32,3 ± 3,8	— 15,4 ± 1,8
A. niger (spores)	— 35,2 ± 3,3	— 12,2 ± 1,4

Measuring the Potential of Aluminum Plates.

Aluminum plates have a negative charge in physiological aqueous solutions. Powdered aluminum oxide is an electropositive sorbent, the excess positive charge of which is generated by Lewis acid sites (**Romanova, Petrova, 2006**). Since the test samples are aluminum plates coated with aluminum oxide, the overall potential of the sample will depend on the negative charge of the aluminum and the positive charge of the coating. Therefore, to calculate the potential of the coating relative to an aqueous solution, it is necessary to measure the potential difference in the aqueous solution between the uncoated aluminum plate and the aluminum plate with the composite coating and subtract this difference.
Table 3 shows that different aluminum alloys have a negative electrical potential relative to the FBR of -545 and -1120 mV. MAO coatings reduce the negative potential of aluminum plates by 145-170 mV, and bonded Al2O powder by 105 mV due to a shift in the potential to the positive side.

Table 3 Electric potentials of aluminum plates from three alloys, without MAO coating and with MAO and Al_2O_3 coating in a phosphate buffer solution with pH 7.4. The mean values and standard deviations for the results of 4 experiments are presented.

Alloy	Potential , mV
D16	–545 ± 12
D16 + MAO	–400 ± 8
Coating MAO	+145 ± 20
AlMg6	–545± 14
AlMg6+ MAO	– 380 ± 7
Coating MAO	+165 ± 21
Zn-Al	–1120± 25
Zn-Al+ MAO	–950± 15
Coating MAO	+170 ± 40
D16	–545 ± 12
D16 + Al_2O_3	–445 ± 7
Al_2O_3	+100 ± 19

Scanning electron microscopy

Scanning electron microscopy (SEM) analysis revealed a heterogeneous distribution of microorganisms across the coated surfaces: localized regions of dense cell accumulation were observed alongside areas with little or no microbial coverage (Fig. 5).
SEM observations of bacterial adhesion on porous Al_2O_3/metal composite surfaces revealed distinct morphological features depending on the microbial species and coating type. *S. aureus* (Fig. 5A) appeared as spherical cocci with diameters of approximately 0.8–1.2 μm, frequently forming diplococci or small clusters. On highly porous coatings, particularly Zn–Al with large pores (10–30 μm), cells were preferentially localized within surface depressions, where they adhered tightly to the rough substrate. In contrast, fewer clusters were observed on Al–Mg6 and D16 coatings, likely due to their smaller pore size. *B. subtilis* (Fig. 5B) was observed as rod-shaped cells approximately 1–2 μm in length, occasionally containing visible spores (oval and more electron-dense structures). Adhesion predominantly occurred within pores, with a higher density of cells observed in the larger pores of Zn–Al coatings. *P. aeruginosa* (Fig. 5C) exhibited slender Gram-negative rod morphology (approximately 1.5–5 μm in length), typically appearing as single cells or short chains. On rough surfaces, cells displayed elongated conformations and were frequently attached to protrusions and pore edges. Zn–Al coatings consistently demonstrated the highest surface cell density. A heterogeneous distribution of bacterial cells was observed across all coating types, characterized by localized accumulation within pores and surface irregularities, while smoother regions remained sparsely populated. This pattern suggests that both mechanical retention within pores and electrostatic interactions contribute to microbial adhesion on MAO-derived surfaces.
The Zn–Al sorbent exhibited the highest sorption capacity for most of the tested cultures, particularly fungi, likely due to the presence of large pores (10–30 μm) and the $ZnO/ZnAl_2O_4$ phases. The sorption efficiency of Zn–Al was approximately 13–15% higher compared to that observed for *Escherichia coli*. In contrast, reduced adsorption of fungal spores was observed on the D16 substrate, possibly due to the presence of γ-Al_2O_3, which possesses bactericidal properties. This phenomenon is supported by literature reports indicating that γ-Al_2O_3 exhibits higher antibacterial activity compared to α-Al_2O_3, potentially due to increased generation of reactive oxygen species (ROS) (**Pakrashi *et al*., 2022; Gudkov *et al*., 2022**).

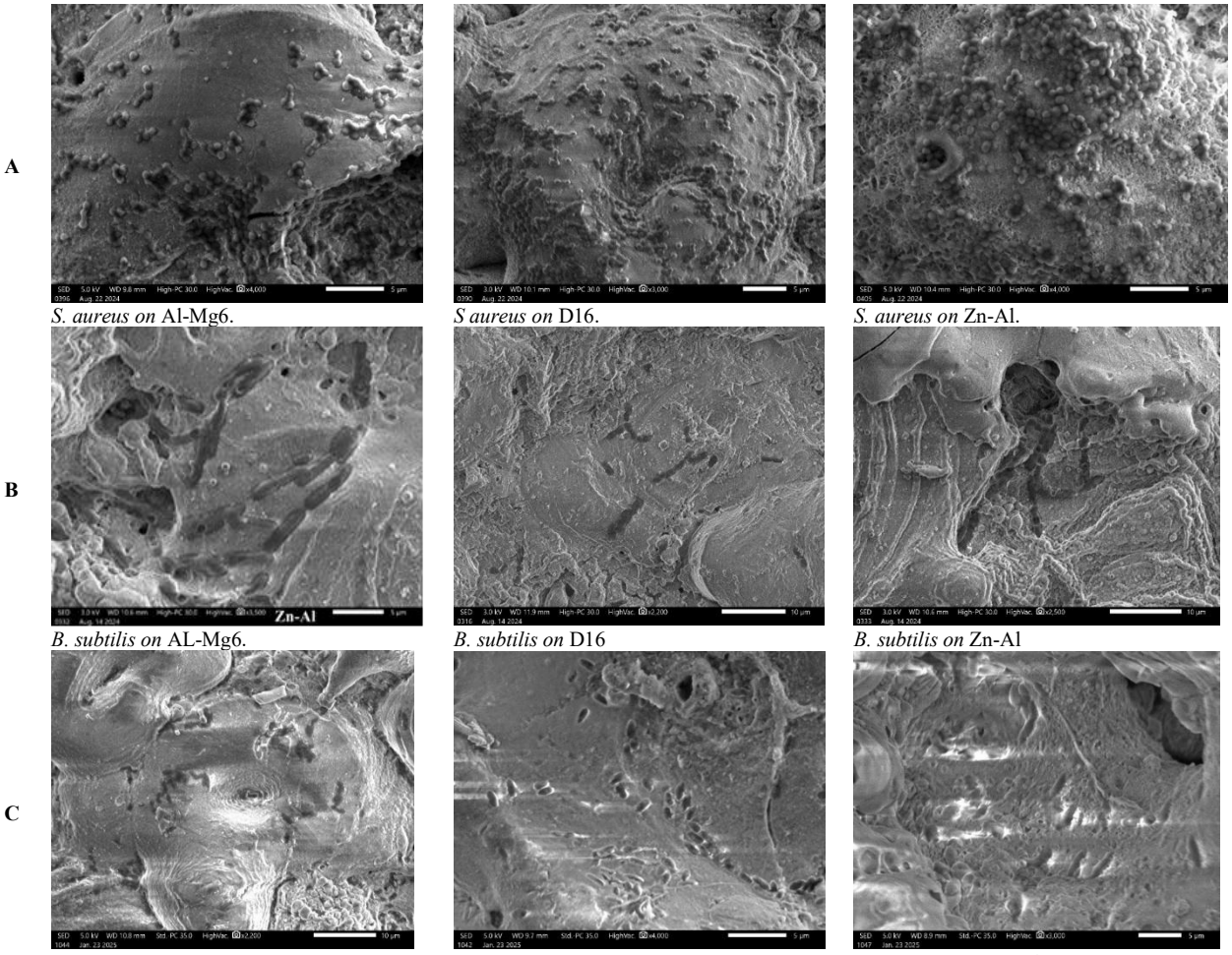

S. aureus on Al-Mg6. *S aureus on* D16. *S. aureus on* Zn-Al.

B. subtilis on AL-Mg6. *B. subtilis on* D16 *B. subtilis on* Zn-Al

P. aeruginosa on AI-Mg6 *P.aeruginosa* on D16 *P. aeuginosa on* ZnAl

Figure 4 Scanning electron micrographs illustrating the adsorption of bacterial cells on composite MAO coatings: (A) *Staphylococcus aureus* (Gram-positive cocci, frequently forming clusters); (B) *Bacillus subtilis* (rod-shaped cells and/or spores); (C) *Pseudomonas aeruginosa* (Gram-negative rods). Coatings are arranged from left to right as Al–Mg6, D16, and Zn–Al. Images were acquired at a magnification of ×4000. Scale bars correspond to 10 μm. SEM parameters: accelerating voltage 5.0 kV and working distance 10.4 mm. Samples were prepared using standard fixation, dehydration, and Au/Pt sputter coating procedures, and analyzed using a JEOL JSM-2100 (JEOL, Japan). *Values represent the mean of three independent experiments with standard deviations indicated.

Figure 5 shows the adsorption of three microorganisms on aluminum plates with composite coatings (Zn–Al, D16, and Al–Mg6). In panel A, *Escherichia coli* cells exhibit a typical rod-shaped morphology with rounded ends. On D16 and Al–Mg6 coatings, a high adsorption density is observed, with the formation of multilayered aggregates. The cell surface appears generally smooth, although slight wrinkling and folding are frequently observed, likely due to dehydration during SEM sample preparation. A dense multilayer structure is evident, where cells are closely attached both to each other and to the surface relief of the coatings, forming clusters and “island-like” structures. This indicates a high adsorption capacity of *E. coli*. Morphological changes associated with different coatings were also observed. On Zn–Al (zinc-containing) surfaces, cells often appeared wrinkled and deformed, with visible indentations or signs of lysis, suggesting damage to the outer membrane. In contrast, on D16 and Al–Mg6 coatings, cell morphology remained closer to the native state, with more regular shapes and better preservation of cellular integrity, while maintaining high adsorption levels.

In panel B, *C. albicans* cells are observed as oval blastoconidia measuring approximately 3–6 μm, with a smooth surface morphology. In panel C, conidiospores of *A. niger* exhibit a spherical shape with a characteristic rough surface; their morphology is best preserved on coatings that do not exhibit pronounced antimicrobial activity.

In contrast, on coatings with antimicrobial properties, particularly Zn–Al, clear signs of cellular damage are observed, including wrinkling, deformation, loss of turgor, and disruption of cell wall or membrane integrity.

Surface porosity and pore size are critical for microbial adhesion. Large pores that accommodate cells increase surface area and microbial adhesion, while pores that do not accommodate cells reduce adhesion and even repel microorganisms **(Kim *et al.* 2015)**.

In our experiments, microbial sorption significantly depends on the pore size distribution of the coatings. Zn–Al coatings with pore sizes of 10–30 μm adsorbed more microbial cells than Al–Mg6 and D16 coatings, whose sizes (0.5–5.0 μm) are comparable to the size of microorganisms. Furthermore, the pore depth in aluminum plates obtained by MAO was approximately 20 μm, so adsorption on them was higher than on bonded alumina. During the experiments, it was observed that spores of the yeast-like fungus C. albicans and the filamentous fungus A. niger adhered differently to the surfaces studied. Among the sorbents, the Zn–Al coating showed the highest level of fungal spore adsorption, followed by the Al–Mg6 coating, while the D16 coating demonstrated the lowest number of adsorbed fungal spores.

Notably, the D16-based sorbent consists exclusively of the hexagonal γ-Al_2O_3 modification of alumina, which is reported to possess bactericidal and antimicrobial properties. The pore sizes of this coating range from 0.5 to 5 μm, with individual pores up to 20 μm. The porosity of the surface layer is 40–50%. The comparatively lower adsorption of fungal spores on D16 may be related to its antimicrobial activity. At the same time, fungal spores—due to their larger size—appear to preferentially attach to the larger pores of the sorbent.

The most preferred sorbent, based on an Al–Mg6 alloy, consists of a combination of cubic α-Al_2O_3 (considered a stable and non-toxic phase) and γ-Al_2O_3 in a ratio of 70% to 30%, with the non-toxic α-phase predominating. The coating thickness is 60–70 μm, the surface porosity is 40–50%, and the pore sizes range from 0.5 to 5 μm. Scanning electron microscopy images (Fig. 4A, B) reveal irregular pores up to 20 μm in size formed at the boundaries of the remelted agglomerates. The porous layer depth is approximately 20 μm, and the total bilateral surface area is 20.5 cm^2. The Zn–Al coating is a heterogeneous sorbent composed of aluminum oxide (α-Al_2O_3), zinc oxide, zinc aluminate ($ZnAl_2O_4$), and aluminosilicate in the form of mullite ($3Al_2O_3$ $2SiO_2$; $Al_6Si_2O_{13}$). The mixed phase structure, the presence of silicon-containing compounds, larger pores (10–30 μm), smaller pores (1–3 μm), and a large total surface area (approximately 23.4 cm^2) likely contribute to the enhanced adhesion of fungal spores observed on this coating (Fig. 6 B, C).

Thus, aluminum plates with a ceramic coating obtained by microarc oxidation can serve as effective sorbents for the immobilization of microorganisms of various taxonomic groups. In the future, they can be used to detect microorganisms in environmental samples, biological fluids, contaminated soils and wastewater, to preserve microbial collections and in various biotechnological processes.

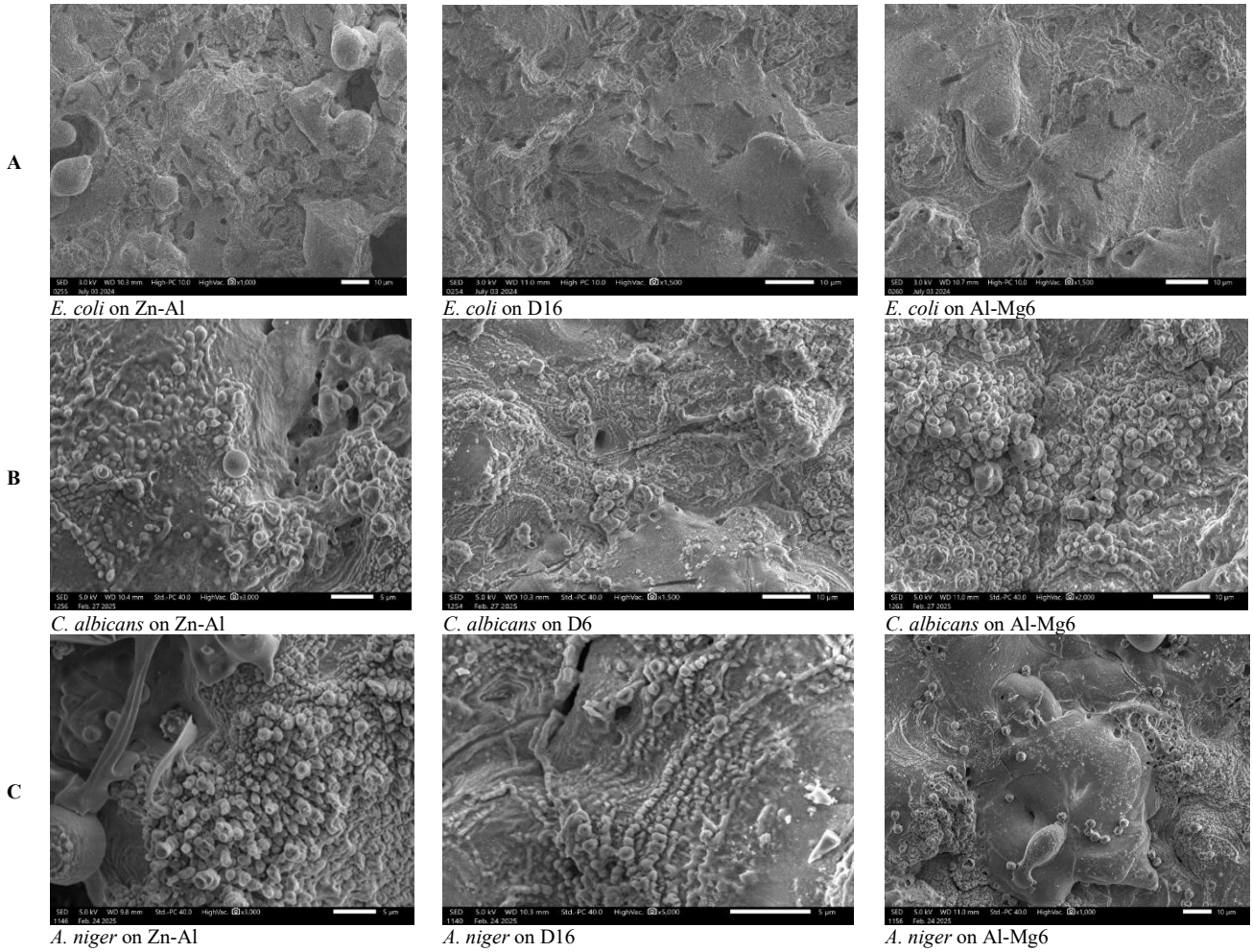

Figure 6 Adsorption of *E. coli* cells (A), *C. albicans* spores (B), and *A. niger* conidiospores (C) on aluminum plates with three types of composite coatings: Zn–Al, D16, and Al–Mg6. White line – 10 µm.

CONCLUSION

Micro-arc oxidation of three types of alloys (Zn–Al, Al–Mg6, and D16) resulted in the formation of composite coatings composed of mullite ($3Al_2O_3 \cdot 2SiO_2$) and various forms of aluminum oxides (α- and γ-Al_2O_3), as well as crystalline and amorphous aluminum–silicon compounds. By targeted modification of the composition and structural features of the coatings, it is possible to achieve a synergistic effect in the adsorption of both chemical substances and microbial cells. Among various sorbents, aluminum oxide remains one of the most widely used materials due to its electropositive nature, arising from Lewis acid sites (coordinatively unsaturated surface aluminum atoms with localized positive charge) (**Romanova and Petrova, 2006**). At the same time, the surface of microbial cell walls carries a negative charge, primarily due to the presence of anionic polymers (**Ferreyra Maillard *et al*., 2021**), which promotes electrostatic interactions between microorganisms and the sorbent surface.

The conducted studies demonstrated that all six investigated indicator microorganisms, belonging to different taxonomic groups, were adsorbed onto composite coatings produced by micro-arc oxidation in accordance with the principles of equilibrium adsorption. Specifically, an increase in microbial concentration in the surrounding medium resulted in a corresponding increase in the number of cells adsorbed onto the sorbent surface until saturation of binding sites was achieved.

Scanning electron microscopy images showed that microorganisms were distributed unevenly on the sorbent surface, with regions of dense adsorption alongside areas containing fewer bacterial cells and fungal spores. Following desorption under physiological conditions, a residual population of cells (not exceeding 5.0×10^3 cells/mm²) remained on the plates, likely due to strong attachment mediated by functional groups of the sorbent interacting with bacterial cells and fungal spores. The adsorption capacity of composite microplasma coatings was several times higher than that of coatings containing immobilized aluminum oxide powder. Furthermore, spherical cocci and fungal spores were found to adsorb to a greater extent than rod-shaped bacteria.

Thus, microorganisms interacting with aluminum oxide surfaces of varying composition and pore size can be effectively retained, primarily due to electrostatic (Coulombic) interactions. The bactericidal properties of aluminum oxide nanoparticles have also been confirmed in several studies (**Gudkov *et al*., 2022; Kazantsev *et al*., 2022**).

Many existing studies focus on the synthesis of aluminum oxide nanoparticles and microparticles for attachment to polymer fibers, which typically involves multistep processes and may result in nanoparticle agglomeration and weak adhesion to substrates (**Larionov *et al*., 2011**). This can lead to particle leaching, reduced efficiency, and limited applicability in analytical applications involving desorption studies. These limitations can be overcome by forming aluminum oxide directly on an aluminum substrate through oxidation. Based on the literature and our experimental results, aluminum plates with microplasma coatings represent promising solid sorbents for microbiological applications, including microbial immobilization, preservation of microbial cultures and metabolites, environmental monitoring, and biotechnological processes requiring stable and insoluble sorbent materials. Furthermore, optimization of the coating composition enhances the synergistic adsorption of both chemical and biological substances, including microbial cells and their metabolites, particularly those exhibiting electrophilic properties.

Overall, all six tested microorganisms in this study demonstrated the ability to adsorb onto composite coatings produced by micro-arc oxidation in accordance with the principles of equilibrium adsorption governed by electrostatic interactions. An increase in microbial concentration led to a proportional increase in adsorption until surface saturation was reached. Following desorption, a fraction of bacterial cells and fungal spores remained strongly attached to the sorbent surface.

Thus, aluminum plates based on Zn–Al, Al–Mg6, and D16 alloys with microplasma coatings can be considered promising next-generation solid sorbents for broad applications in microbiology, biotechnology, as well as in various industrial and engineering fields.

REFERENCES

Abdullaev, Kh. (2023). Mechanisms of the action of metal ions on microbes.*Tashkent Journal of Biotechnology*, (2),45–52.

Borisov, A., Krit, B.L., Lyudin, V.B., Morozova, N.V. *et al*. (2016). Microarc oxidation in slurry electrolytes:A review,*Surface Engineering and Applied Electrochemistry,* V.52, p.50.

Danat B.T.,Wuana R.A.,Chahul H.,F.,Iorungwa M.S.(2026).Review of adsorption isotherms models.*Applied Water Science.*16:72. https://doi.org/10.1007/s13201-025-02682-0

Davis,J.R.(2001). Aluminum and aluminum alloys.In J.R.Davis (Ed.),*Alloying:Understanding the basics* (pp.351–416).ASM International. https://doi.org/10.1361/autb2001p351

Ferreyra Maillard, A.P.V.,Espeche,J.C.,Maturana,P.,Cutro,A.C.*et al*.(2021).Zeta potential beyond materials science:Applications to bacterial systems and to the development of novel antimicrobials.*Biochimica et Biophysica Acta (BBA) - Biomembranes*,v.1863,183597. https://doi.org/10.1016/j.bbamem.2021.183597

Gudkov, S.V.,Burmistrov,D.E.,Smirnova,V.V.,Semenova,A.A.,& Lisitsyn,A.B.(2022).A mini review of antibacterial properties of Al2O3 nanoparticles.*Nanomaterials,12*(15),2635.https://doi.org/10.3390/nano12152635

Gupta, M.(2018).Changing wisdom of metallic alloys development. *Materials Sciences and Applications,9*,1021–1035. https://doi.org/10.4236/msa.2018.913074

Hobbie, J.E.,Daley,R.J.,Jasper,S.(1977).Use of Nuclepore filters for counting bacteria by fluorescence microscopy,*Appl.Environ.Microbiol,*v.33,p.1225.https://doi.org/10.1128/aem.33.5.1225-1228.1977

Jwad, K.H., Saleh, T.H.,& Abd-Alhamza,B.(2019).Preparation of aluminum oxide nanoparticles by laser ablation and a study of their applications as antibacterial and wound healing agent.*Nano Biomedicine and Engineering,11*(3),313–319.https://doi.org/10.5101/nbe.v11i3.p313-319

Karamysheva,Y.S.,Komarov,A.I.,Gudkov,V.G.,Orda,D.V.,& Iskandarova,D.O.(2019).Sorption activity of various forms of aluminum oxide against pathogens of parasitic intestinal infections.*Medical News*,(12),68–72.

Kazantsev,S.O.,Bakina,O.V.,Pervikov,A.V.,Rodkevich,N.G.,Quang,N.H.,Le Thi,L.A.,Timofeev,S.S.,& Lozhkomoev,A.S.(2022).Antimicrobial activity and sorption behavior of Al2O3/Ag nanocomposites produced with the water oxidation of bimetallic Al/Ag nanoparticles. *Nanomaterials,12*(21),3888.https://doi.org/10.3390/nano12213888

Komarov,A.I.,Romanyuk,A.S.,& Shipalov,D.A.(2021).Formation of a zirconium dioxide-modified coating on aluminum alloys by micro-arc oxidation in an electrolyte-suspension.*Actual Issues of Mechanical Engineering*,(10),342–345.

Komarov,A.I.,Orda,D.V.,Chernyavskaya,A.S.,Sosnovskiy,A.V.,& Shipalov,D.A.(2024).Structure and prospects of using porous oxidized aluminum as an adsorbent.*Mechanics of Machines,Mechanisms and Materials,2*(67),88–95.https://doi.org/10.46864/1995-0470-2024-2-67-88-95

Kim,S.,Zhou,Y.,Cirillo,J.D.,Polycarpou,A.A.,*et al*.(2015).Bacteria repelling on highly-ordered alumina-nanopore structures.*Journal of applied physics.*v.117,No.15,155302.https://doi.org/10.1063/1.4918305.

Larionov,I.V.,Rybalchenko,O.V.,Orlova,O.G.,Potokin,I.L.,Sushko,T.P.,Khrushcheva,T.A.,Boldyrev,A.G.,&Bondarenko,V.M.(2011). Adsorption of probiotic bacteria on cellulose sorbents. *Sorption and Chromatographic Processes, 11*(6), 848–854.

Lemire,J.A.,Harrison,J.J.,& Turner,R.J.(2013).Antimicrobial activity of metals:Mechanisms,molecular targets and applications.*Nature Reviews Microbiology,11*(6),371–384.https://doi.org/10.1038/nrmicro3028

Li,B.,& Logan,B.E.(2004).Bacterial adhesion to glass and metal-oxide surfaces.*Colloids and Surfaces B:Biointerfaces,36*(2),81–90. https://doi.org/10.1016/j.colsurfb.2004.05.006

Liu Y.,Wang J.*Editors* (2009).*Fundamentals and applications of biosorption isotherms,kinetics and thermodynamics*.Nova Science Publishers, Inc.New York.http://www.novapublishers.com

Mahesh,P.P.,Kolape,J.,Sultana,H.,Neelakanta,G.(2025).McFarland Standards-Based Spectrophotometry Method for Calculating Approximate Multiplicity of Infection for an Obligate Intracellular Bacterium *Anaplasma phagocytophilum*,*Microorganisms,*v.13,662. https://doi.org/10.3390/microorganisms13030662

Manikandan,V.,Jayanthi,P.,Priyadharsan,A.,Vijayaprathap,E.,Anbarasan,P.M.,& Velmurugan,P.(2019).Green synthesis of pH-responsive Al_2O_3 nanoparticles:Application to rapid removal of nitrate ions with enhanced antibacterial activity. *Journal of Photochemistry and Photobiology A: Chemistry,371*,205–215.https://doi.org/10.1016/j.jphotochem.2018.11.009

Pishchikov,G.B.,& Minukhin,L.A.(2017).Adsorption of microorganisms on solid sorbents in continuous biotechnological apparatuses. *Agrarian Bulletin of the Urals*,(12-1),65–69.

Romanova,R.G.,& Petrova,E.V.(2006).Acid-base properties of the surface of aluminum oxides.*Herald of Kazan Technological University*,(6), 73–90.

Srinivasan,N.,Kannan,J.C.,& Satheeskumar,S.(2015).Antifungal activity of pure and aluminium doped zinc oxide nanoparticles against *Aspergillus niger* and *Aspergillus flavus*.*International Journal of PharmTech Research,7*,287–290.

Subramaniam,V.D.,Ramachandran,M.,Marotta,F.,Banerjee,A.,Sun,X.F.,& Pathak,S.(2019).Comparative study on anti-proliferative potentials of zinc oxide and aluminium oxide nanoparticles in colon cancer cells.*Acta Bio Medica,90*(2),241–247.https://doi.org/10.23750/abm.v90i2.6939

Suminov,I.V.,Belkin,P.N.,Epel'fel'd,A.V.,Lyudin,V.B.,Krit,B.L.,& Borisov,A.M.(2011).*Plasma-electrolytic modification of the surface of metals and alloys* (Vol.2).Tekhnosfera.

Suryavanshi,P.,Pandit,R.,Gade,A.,Derita,M.,Zachino,S.,& Rai,M.(2017).*Colletotrichum sp*.-mediated synthesis of sulphur and aluminium oxide nanoparticles and its in vitro activity against selected food-borne pathogens.*LWT – Food Science and Technology,81*,188–194. https://doi.org/10.1016/j.lwt.2017.03.038

Uppal,H.,Kayal,N.,Chawla,S.,Tripathy,S.S.,Gupta,S.,Singh,R.,Sharma,B.,& Singh,N.(2017).Surface modified alumina compact:A potential material for decontamination of trivalent and hexavalent chromium and growth inhibitor of microbes from water.*Advanced Materials Letters, 8*(5),592–599.https://doi.org/10.5185/amlett.2017.6475

Wen,X.,Liu,Y.,Xi,F.,Zhang,X.,& Kang,Y.(2023).Micro-arc oxidation (MAO) and its potential for improving the performance of titanium implants in biomedical applications.*Frontiers in Bioengineering and Biotechnology,11*,1282590.https://doi.org/10.3389/fbioe.2023.1282590

Zhang,T.,Wang,J.,Zhang,G.,& Liu,H.(2020).The corrosion promoting mechanism of Aspergillus niger on 5083 aluminum alloy and inhibition performance of miconazole nitrate.*Corrosion Science,176*,108930.https://doi.org/10.1016/j.corsci.2020.108930